

Rice SVP-group MADS-box proteins, OsMADS22 and OsMADS55, are negative regulators of brassinosteroid responses

Shinyoung Lee, Sang Chul Choi and Gynheung An*

Department of Life Science and National Research Laboratory of Plant Functional Genomics, Pohang University of Science and Technology (POSTECH), Pohang 790-784, Korea

Received 29 September 2007; revised 27 November 2007; accepted 6 December 2007.

*For correspondence (fax +82 54 279 0659; e-mail genean@postech.ac.kr).

Summary

Most short vegetative phase (SVP)-group MADS-box genes control meristem identity and flowering time. Among the three SVP-group genes in rice, OsMADS47 has been reported as a negative regulator of brassinosteroid (BR) responses. Here, we investigated the functional roles of two close homologs, OsMADS22 and OsMADS55, by generating single, double and triple RNAi lines and overexpression lines. Analyses of the plants showed that their roles in regulating meristem identity are well conserved; however, the involvement of these genes in determining flowering time has diversified. Most importantly, OsMADS55 works as a major negative regulator of BR responses, and OsMADS22 functions to support OsMADS55. Whereas single *OsMADS55* RNAi plants display weak BR responses in the lamina joint (LJ), *OsMADS22-OsMADS55* double and *OsMADS22-OsMADS47-OsMADS55* triple RNAi plants manifest dramatic BR responses with regard to LJ inclination, coleoptile elongation and senescence. Stem elongation is also notably reduced in the double and triple RNAi plants, probably because of BR oversensitivity. Expression analyses indicate the diversified roles in age-dependent BR responses. Altogether, our study demonstrates that all three rice SVP-group genes work as negative regulators of BR responses, but that their spatial and temporal roles are diversified.

Keywords: brassinosteroid response, MADS, OsMADS22, OsMADS55, rice, short vegetative phase.

Introduction

The MADS-box gene family is found ubiquitously in living organisms and encodes transcription factors with a conserved DNA-binding domain, called the MADS box. This family is enriched in plant genomes, encompassing about 100 and 70 genes in *Arabidopsis thaliana* (hereafter *Arabidopsis*) and rice, respectively (Arora *et al.*, 2007; Nam *et al.*, 2004). Short vegetative phase (SVP)-group MADS-box genes were first identified as flowering regulators in *Arabidopsis*, and then as modulators of meristem identity in various species.

In *Arabidopsis*, two members of the SVP group regulate flowering in an antagonistic manner: SVP acts as a flowering repressor (Hartmann *et al.*, 2000) and AGAMOUS-like 24 (AGL24) acts as a flowering activator (Michaels *et al.*, 2003; Yu *et al.*, 2002). Recently, SVP has been identified as a flowering repressor mediated by ambient temperature (Lee *et al.*, 2007). Double-mutant analyses have elucidated that *svp* is epistatic to *agl24* (Gregis *et al.*, 2006). However, in the

regulation of floral meristem identity, the two genes perform similar roles. Transgenic plants overexpressing SVP or AGL24 have floral abnormalities (Yu *et al.*, 2004). Moreover, both genes suppress AGAMOUS (AG) by recruiting a co-repressor complex along with APETALA1 (Gregis *et al.*, 2006).

Studies with other dicotyledonous species have revealed conserved roles for these SVP-group MADS-box genes in both floral transition and meristem identity. The tomato *jointless* mutant, which was first identified as a mutant with defective joints (Mao *et al.*, 2000), shows delayed flowering and develops a greater number of leaves (Szymkowiak and Irish, 2006). Additionally, this mutant forms abnormal reproductive structures containing both flowers and leaves, and the flowers often revert to vegetative sympodial growth (Szymkowiak and Irish, 2006). In *Antirrhinum*, INCOMPOSITA controls prophyll development, floral meristem identity and flowering time (Masiero *et al.*, 2004). When *StMADS16*

from *Solanum tuberosum* is ectopically expressed in tobacco, plants exhibit a deferred flowering time and greater node numbers under short-day conditions only (Garcia-Maroto *et al.*, 2000). Furthermore, those transformants confer vegetative features to the flowers.

In contrast, MADS-box genes from monocots mainly regulate meristem identity. In winter wheat, *Triticum aestivum vegetative to reproductive transition-2* (*TaVRT2*) is upregulated during the vegetative phase and is repressed by vernalization, suggesting that this gene functions as a putative repressor of floral transition (Kane *et al.*, 2005, 2007). In barley (*Hordeum vulgare*), ectopic expression of *Barley MADS1* (*BM1*) or *BM10* inhibits spike development and causes floral reversion (Trevaskis *et al.*, 2007). Head emergence is delayed in *BM1* transformants, but expression of the barley *VRN1* gene is not affected. Finally, ectopic expression of *OsMADS22* in transgenic rice plants results in aberrant floral morphogenesis, characterized by a disorganized palea, an elongated glume and a two-floret spikelet (Sentoku *et al.*, 2005).

Roles for SVP-group MADS-box genes in shoot development and brassinosteroid (BR) signaling have also been described in *Paulownia kawakamii* and rice (Duan *et al.*, 2006; Prakash and Kumar, 2002). A deficiency in a rice SVP-group member, *OsMADS47*, leads to shorter primary roots, elongated coleoptiles and enhanced lamina joint (LJ) inclination, indicating that *OsMADS47* is a negative regulator of BR signaling (Duan *et al.*, 2006). Here, we elucidated the roles of two other SVP-group MADS-box genes (*OsMADS22* and *OsMADS55*) plus *OsMADS47*, using single, double and triple knock-down mutants.

Results

Expression patterns of SVP-group MADS-box genes in rice

The rice genome contains three SVP-group MADS-box genes (*OsMADS22*, *OsMADS47* and *OsMADS55*), compared with two members in Arabidopsis (*SVP* and *AGL24*) (Lee *et al.*, 2003). On the phylogenetic tree, *OsMADS47* is grouped with *SVP*, whereas *OsMADS22* and *OsMADS55* are clustered with *AGL24*. *OsMADS47* showed 49.8% identity with *SVP*, whereas *OsMADS22* and *OsMADS55* had 47.0% and 45.6% identity, respectively, with *AGL24* when the BLOSUM62 matrix was used. Meanwhile, *OsMADS22* showed 79.1% identity and 81.0% similarity to *OsMADS55*.

Because SVP-group MADS-box genes act as flowering regulators in Arabidopsis, we checked this possibility by examining their RNA transcript levels. Expression of *Ehd1* and *Hd3a*, both short day (SD)-preferential promoters, is higher under SD conditions than under long-day conditions (LD) (Doi *et al.*, 2004; Kojima *et al.*, 2002). Transcript levels of *OsMADS50* and *OsMADS14*, which generate positive flowering signals, increase as plants age (Jang *et al.*, 2002; Lee

et al., 2004). Therefore, if the SVP-group MADS-box genes are flowering regulators, expression of these genes may differ between SD and LD, or else change when floral transition occurs. In the Dongjin cultivar studied here, heading takes place under SD after about 75 days post-germination, and after 95 days under LD (Kim *et al.*, 2007). Thus, because the floral transition happens approximately 30 days before heading, we sampled leaf blades from 45-day-old plants and found that all three rice SVP-group members were expressed at the same level under either SD or LD conditions (Figure 1a). This suggests that the genes are not involved in photoperiod-dependent flowering regulation. We also observed no difference when real-time PCR analyses were performed for 55-day-old leaves (data not shown).

However, temporal expression patterns did vary among these genes. Although *OsMADS47* transcript levels decreased as the plants grew, those of *OsMADS55* increased at leaves became older (Figure 1b), whereas the level of *OsMADS22* mRNA remained constant throughout all stages. Therefore, it appears that *OsMADS47* is preferentially functional in young stages, whereas *OsMADS55* plays major roles in older stages. In contrast, in roots, expression levels of all three genes increased as plants aged, suggesting that they all regulate root development in a synergistic manner (Figure S1a). We divided 5-day-old seedlings into three parts – roots, shoots and coleoptiles – in order to determine the organ-dependent roles of these genes. In coleoptiles, the transcript level of *OsMADS22* was higher than that of *OsMADS47* and *OsMADS55*, whereas in roots and shoots the *OsMADS47* transcript was the most abundant, implying diversified roles of SVP-group genes (Figure S1b).

OsMADS47 is a negative regulator of BR signaling (Duan *et al.*, 2006). We studied whether expression of the SVP-group genes is influenced by BR or gibberellin (GA_3). As a positive marker for BR treatment, we selected *DWARF2*, which is downregulated by BR (Hong *et al.*, 2003). Three-week-old seedlings were treated for 12 h with either 1 μ M epibrassinolide (BL) or 30 μ M GA_3 . As expected, *DWARF2* was down-regulated by BL, but the levels of the SVP-group MADS-box transcripts were not changed significantly (Figure 1c). Similar results were obtained with 10 μ M BL (data not shown). Similarly, GA_3 did not affect their expression. We also treated seedlings with 1 μ M BL for 5 days following germination. Analyses of the seedlings as a whole did not reveal any significant difference in expression levels (Figure 1d), thereby suggesting no direct regulation by BL.

OsMADS22 knock-out plants did not show any visible defects

To elucidate the *in vivo* function of *OsMADS22* and *OsMADS55*, we searched for insertional mutants from our transferred DNA (T-DNA) flanking sequence database (An *et al.*, 2003; Jeong *et al.*, 2006). For *OsMADS22*, two lines

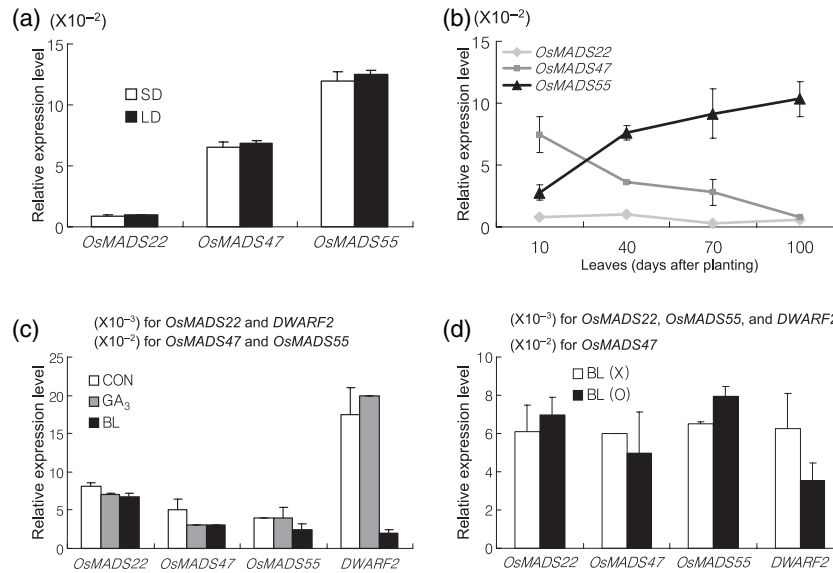


Figure 1. Expression of SVP-group MADS-box genes. The y-axis represents relative values between the transcript levels of the target genes and the *Ubiquitin* control. Each data point is the average of two or three independent real-time PCR analyses.

(a) Photoperiod-dependent expression patterns. Light conditions were 10-h light/14-h dark for short days (SD) and 14-h light/10-h dark for long days (LD). Leaf blades were sampled from 45-day-old plants.

(b) Developmental stage-dependent expression patterns. The uppermost leaves were sampled at each developmental stage.

(c) Hormone effects. Three-week-old seedlings were treated with 30 μM gibberellin (GA_3) or 1 μM epibrassinolide (BL) for 12 h.

(d) Constitutive brassinosteroid (BR) effects. Seedlings were grown for 5 days from germination on media containing 1 μM BL.

were identified in which T-DNA was inserted into the third exon (line 2D-41659) or the fourth intron (line 2C-40478) (Figure S2a). These alleles were designated as *osmads22-1* (22KO1) and *osmads22-2* (22KO2). Both are considered null alleles because *OsMADS22* transcripts were not detected (Figure S2c). Homozygous plants showed no significant phenotypic changes in flowering time, height or LJ inclination (Table S1 and Figure S2b).

Suppression of OsMADS55 expression caused a reduction in the number of elongated internodes and an increase in LJ inclination

No T-DNA insertion line exists for *OsMADS55*. Therefore, we generated transgenic plants expressing *OsMADS55* RNAi transcripts under the control of the *ubiquitin (Ubi)* promoter using the pANDA vector (Miki and Shimamoto, 2004). Nine transgenic lines (55R plants) were analyzed; all exhibited strong reductions in *OsMADS55* transcript levels, whereas those of *OsMADS22* and *OsMADS47* were comparable with the wild-type (WT) plants (Figure 2a).

One of the most notable phenotypes of the 55R plants was an increased LJ inclination (Figure 2c). In the flag leaves (the first leaves), the LJ angles of 55R plants were larger than those of the controls. In comparison, the second leaves showed some, but not significant, change in the LJ inclination (Figure 2c). This suggests a negative role for *OsMADS55* in the BR response because BR acts positively in that process.

Because BR is associated with stem elongation, we analyzed these patterns in detail. Although the plant height was unchanged (Figure 2b), the transgenic plants had fewer elongated internodes (Figure 2d). For the control, the average number of elongated internodes was 5.0, compared with 4.2 for the 55R plants (Figure 2d). In contrast, the number of such internodes on the *osmads22* knock-out plants did not differ from the control (Table S1).

Co-suppression of OsMADS22 and OsMADS55 caused severe height reductions and increased LJ angles

Because the knock-down of *OsMADS22* expression did not prompt any phenotypic changes, whereas a reduction in *OsMADS55* expression did affect plant development, we postulated that *OsMADS22* might perform a redundant role in assisting *OsMADS55*. To examine this possibility, we took a double RNAi approach to knock-down *OsMADS22* and *OsMADS55* simultaneously. The transformants (2255R plants) expressing both *OsMADS22* and *OsMADS55* RNAi transcripts showed severe phenotypes compared with the 55R plants (Figure 3a). Among the 22 primary transgenics, 20 had significant changes in their LJ inclination and height. In some plants, the panicles did not emerge from the flag leaves because of severe stem reductions. When RT-PCR analyses were performed for 11 lines, *OsMADS22* and *OsMADS55* transcript levels were significantly reduced in the lines with abnormal phenotypes (Figure S3).

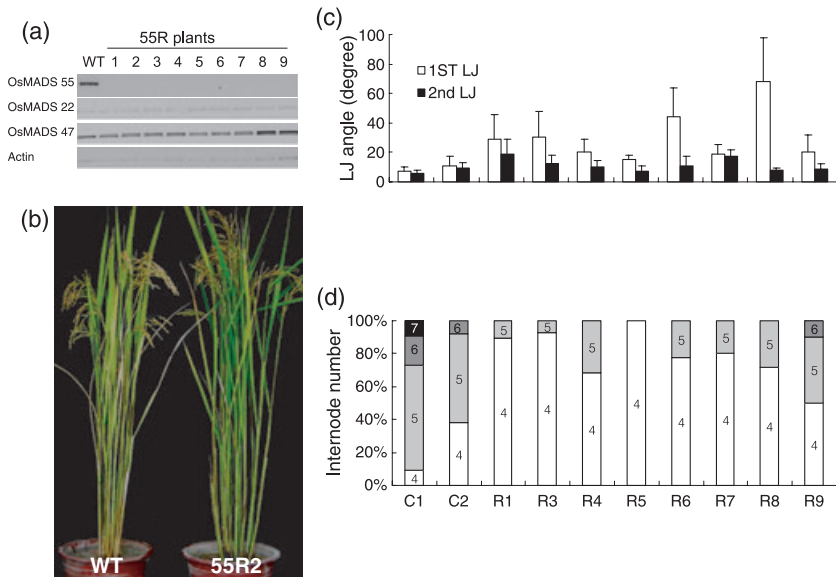


Figure 2. Phenotypes of transgenic plants. (a) RT-PCR analyses of transgenics suppressing *OsMADS55* (55R plants). The numbers indicate the independent transformants. (b) Photograph of wild-type (WT) and 55R #2 plants at the mature stage. (c) Angle of lamina joint (LJ) inclination in 55R plants (7–10 leaves analyzed): 1st LJ, LJ of flag leaf; 2nd LJ, LJ of leaf below flag leaf. Transgenic plants transformed with an empty vector were used as controls (C1 and C2). (d) Distribution of elongated internodes in 55R plants (7–10 stems analyzed). The same plants examined for (c) were used here.

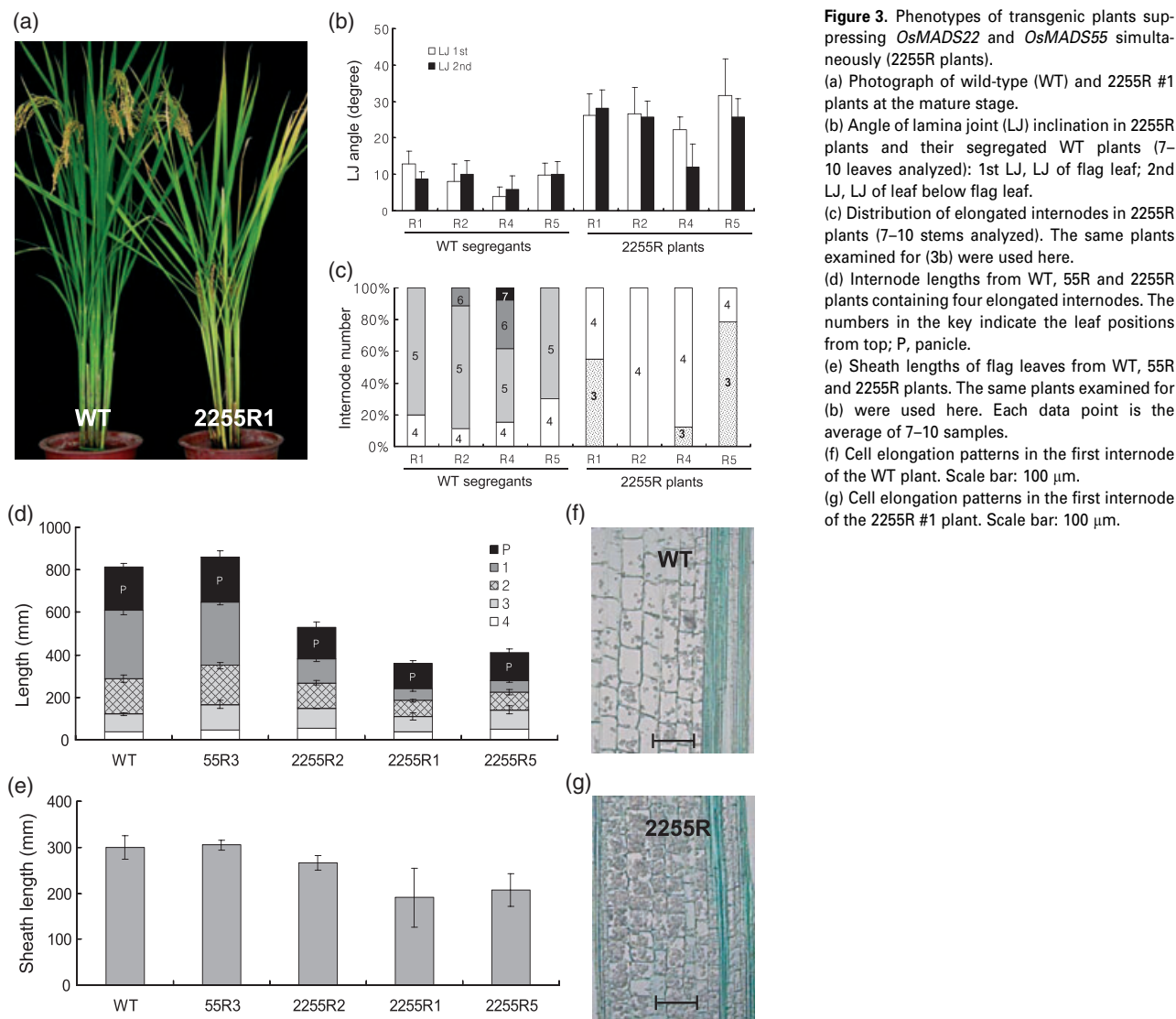


Figure 3. Phenotypes of transgenic plants suppressing *OsMADS22* and *OsMADS55* simultaneously (2255R plants). (a) Photograph of wild-type (WT) and 2255R #1 plants at the mature stage. (b) Angle of lamina joint (LJ) inclination in 2255R plants and their segregated WT plants (7–10 leaves analyzed): 1st LJ, LJ of flag leaf; 2nd LJ, LJ of leaf below flag leaf. (c) Distribution of elongated internodes in 2255R plants (7–10 stems analyzed). The same plants examined for (3b) were used here. (d) Internode lengths from WT, 55R and 2255R plants containing four elongated internodes. The numbers in the key indicate the leaf positions from top; P, panicle. (e) Sheath lengths of flag leaves from WT, 55R and 2255R plants. The same plants examined for (b) were used here. Each data point is the average of 7–10 samples. (f) Cell elongation patterns in the first internode of the WT plant. Scale bar: 100 μ m. (g) Cell elongation patterns in the first internode of the 2255R #1 plant. Scale bar: 100 μ m.

Four lines (R1, R2, R4 and R5) were selected for further analysis in the next generation. The transgenic plants manifested increased LJ inclination both in the first and the second leaves (Figure 3b), with average angles of 32° and 24°, respectively, compared with 8.6° and 8.7°, respectively, for the WT segregants. Transformed plants were shorter than the WT: 466 mm versus 951 mm (Table S1). To understand the nature of this significant height reduction, we analyzed two aspects of the transgenic plants. First, their stems had fewer elongated internodes (average 3.6) compared with the distribution on the control stems (average 5.0; Figure 3c). Second, the internode lengths, especially for the first and second internodes, were reduced, sometimes significantly, in the 2255 RNAi plants (Figure 3d). In contrast, the 55R plants did not show changes in the internode length (Figure 3d). We also observed that the flag leaf sheaths were shorter on the 2255 RNAi plants than on the control (Figure 3e). Longitudinal sections of the first internodes indicated that cell elongation was suppressed in the transgenic plants (Figure 3f,g). Finally, the lengths of the flag leaf blades were slightly reduced on the 2255R plants, although the lengths of sheaths and blades on the leaves below the flag leaves were unchanged (data not shown). Furthermore, the double RNAi plants displayed enhanced senescence (Figure 3a), whereas the 22KO and 55R plants did not show any senescence phenotype at the similar developmental stage. Therefore, our double RNAi experiment demonstrated that OsMADS22 assists the functioning of OsMADS55 in the LJ inclination, stem elongation and senescence processes.

We also performed quantitative real-time PCR analyses to verify that the phenotypes observed from the transgenic plants were not the result of cross-suppression of other members (Figure 4a). In 55R transgenic plants, *OsMADS55* transcript levels were greatly reduced. However, the transcript levels of *OsMADS47* were not significantly altered, whereas those of *OsMADS22* were unchanged in line 1 but decreased in line 3. Because the angle of LJ inclination was almost the same in these two lines, it must have resulted from the reduction in *OsMADS55* transcripts (Figure 4b).

In 2255R double RNAi plants, the transcript levels of *OsMADS22* and *OsMADS55* were significantly less, whereas the levels of *OsMADS47* were only mildly affected. These plants also exhibited additional phenotypes (e.g. reduced heights and an increase in the LJ angle in their second leaves; Figure 4b,c). Therefore, these phenotypes resulted from the simultaneous loss of both *OsMADS22* and *OsMADS55*.

Suppression of all three SVP-group MADS-box genes caused severely reduced stem elongation and increased LJ inclination

We used the RNAi approach to regenerate triple knock-down transgenic plants (224755R) that suppressed the expressions of *OsMADS22*, *OsMADS47* and *OsMADS55*. Except for

line 9, which had normal heights and LJ angles, transcript levels of the SVP-group genes were significantly reduced in the other 11 transgenic plants (Figure 4d). These lines also had increased LJ angles at their flag leaves (Figure 4e). In addition, the LJ angle of the second leaves was significantly increased, and the plant height was reduced in most of those lines (Figure 4e,f).

In the first and second leaves, the angle of LJ inclination in the triple RNAi plants was comparable with those in the 2255R plants, suggesting that *OsMADS47* does not additively enhance LJ inclination. Although the average angles of LJ inclination of the 2255R plants were $29.0 \pm 3.9^\circ$ (1st LJ) and $27.0 \pm 1.8^\circ$ (2nd LJ) (Figure 4b), those of the triple RNAi lines (2, 4, 5 and 12) were $31.2 \pm 4.7^\circ$ (1st LJ) and $27.4 \pm 1.2^\circ$ (2nd LJ) (Figure 4e). These RNAi lines were selected for comparison because they displayed a similar level of transcription suppression of *OsMADS22* and *OsMADS55*. Similarly, the plant heights were not further reduced in the triple knock-down plants (398.3 ± 50.5 mm) compared with the double knock-down 2255R plants (402.5 ± 0.7 mm). This indicates that *OsMADS47* is not likely to be involved in controlling stem elongation. In 224755R, lines 6 and 11, heights were nearly normal and the *OsMADS55* transcript level remained relatively high in those plants. This observation supports the theory that the stem elongation process is mainly dependent on the level of *OsMADS55*. However, because suppression of *OsMADS55* alone did not affect the height, a simultaneous suppression of *OsMADS22* was needed for inhibiting stem elongation.

OsMADS22 overexpression plants produced shortened panicles and stems

To further characterize the functioning of *OsMADS22*, we made transgenic plants that over-expressed full-length cDNA under the control of the *Ubi* promoter. Among the 43 transformants overexpressing *OsMADS22* (22OX plants), fertility was reduced in 39 lines, and panicles and upper stems were shorter in 36 lines (Figure 5a,b). Some lines also had flower defects, including an undeveloped palea and elongated glume; these had been described previously by Sentoku *et al.* (2005) (data not shown). We also observed that senescence was delayed in the overexpression plants (Figure 5c), and that the angle of LJ inclination was decreased in the first and second leaves (Figure 5d). The extent of the altered phenotypes was correlated with the level of the *OsMADS22* transcript (Figure 5e).

OsMADS55 overexpression induced stem elongation

Out of the 28 transgenic plants that overexpressed *OsMADS55* (55OX), two showed normal phenotypes, whereas the rest displayed low fertility, abnormal florets (Figure S4), shortened panicles (Figure 6a) and elongated

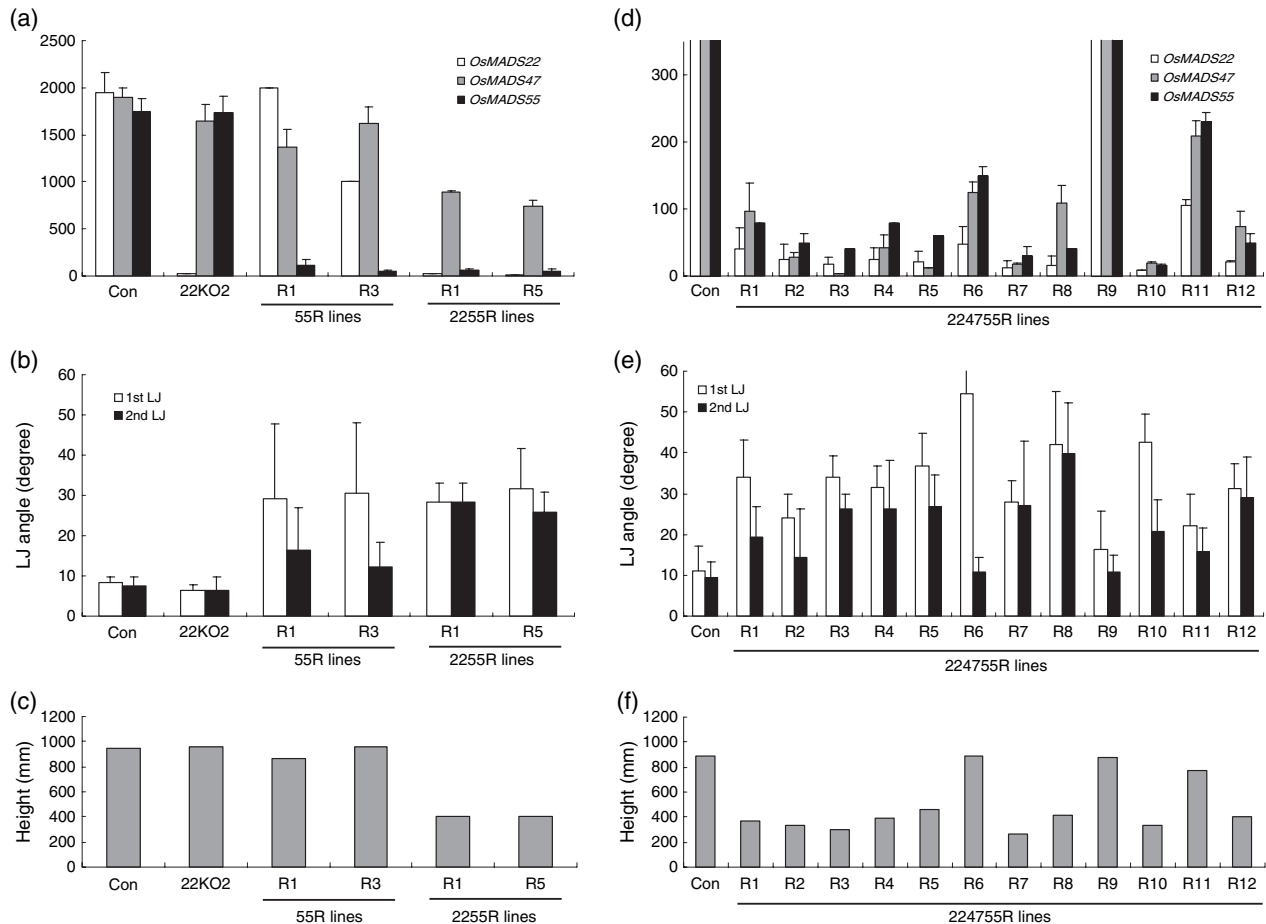


Figure 4. Quantitative analyses for 22KO, 55R, 2255R and OM224755R transgenic plants. In (a) and (b), real-time PCR analyses were performed twice for each sample. Levels of expression relative to *ubiquitin* were measured for each gene, and were adjusted to similar levels in control plants. The y-axis gives artificial units. Controls were wild-type (WT) segregants of the 22KO2 (a–c) and T₁ plants transformed with empty vector and showing normal phenotype (d–f).

(a) Relative expression levels of the short vegetative phase (SVP)-group MADS-box genes in 22KO, 55R and 2255R plants.

(b) Angle of lamina joint (LJ) inclination from 22KO, 55R and 2255R plants: 1st LJ, LJ of flag leaf; 2nd LJ, LJ of leaf below flag leaf.

(c) Heights of 22KO, 55R and 2255R plants.

(d) Relative expression levels of SVP-group MADS-box genes in 224755R plants.

(e) Angle of LJ inclination from 224755R plants: 1st LJ, LJ of flag leaf; 2nd LJ, LJ of leaf below flag leaf.

(f) Heights of 224755R plants.

stems (Figure 6c,d), with the last feature resulting from an increase in the number and length of elongated internodes (Figure 6b). Whereas the transgenics exhibited an average of 5.9 elongated internodes, the controls had an average of 4.9. Internodes on the transgenics were longer at all positions except the panicle (Figure 6c). Similar phenotypes were observed in the next generation. In addition, senescence was significantly delayed (Figure 6d).

To investigate the process of altered elongation in the 55OX plants, we compared their stems with those of 2255R and the WT. At 75 days after planting (DAP), when the fifth internode was beginning to elongate in the WT, the sixth internode had already started elongating in the 55OX plants (Figure 7a), whereas the 2255R plants were about to elongate at just their fourth internode. At 97 DAP, the internodes were longer on the 55OX plants than on the WT, and an

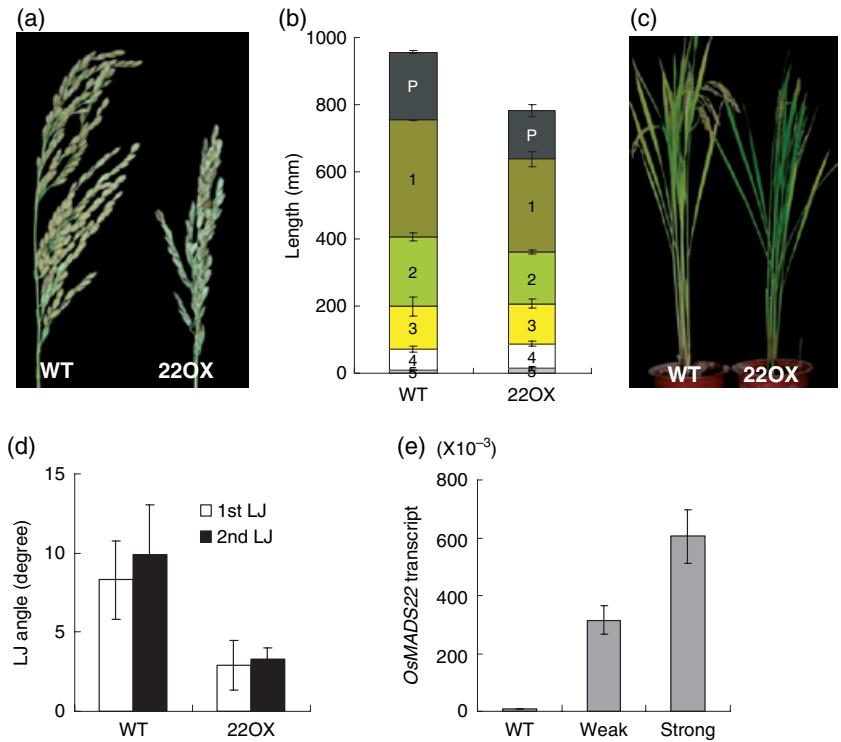
additional sixth internode had developed on the 55OX plants (Figure 7b). When the WT and 2255R panicles were at the early stage of secondary rachis-branch primordial differentiation, and were developing bract hairs, the panicles of the 55OX plants were only at the primary stage for rachis-branch primordial differentiation (Figure 7c, lower panel). Nevertheless, even though the staging was similar between WT and 2255R plants, the panicle primordia were smaller in 2255R plants (Figure 7c, lower panel), reflecting the reduction in panicle size after maturation (Figure 3f).

The molecular nature of increased LJ inclination in RNAi transgenic plants

In lines from 55R, 2255R and 224755R, LJ inclinations were increased. Because BR is a well-known positive regulator of

Figure 5. Phenotypes of transgenic plants over-expressing *OsMADS22*.

(a) Panicle morphology for wild-type (WT) segregant (left) and homozygous *OsMADS22*-over-expressing plant of line 6 (22OX).
 (b) Stem elongation patterns from WT and 22OX plants containing five elongated internodes. The numbers indicate the internode positions from top; P, panicle.
 (c) Phenotypes for WT and 22OX plants.
 (d) Angle of lamina joint (LJ) inclination of 22OX plants and their segregated WT: 1st LJ, LJ of flag leaf; 2nd LJ, LJ of leaf below flag leaf.
 (e) *OsMADS22* transcript levels in LJ regions, sampled from T₂ segregants showing WT-like, weak or strong phenotypes. Each data point is the average of two independent segregants.



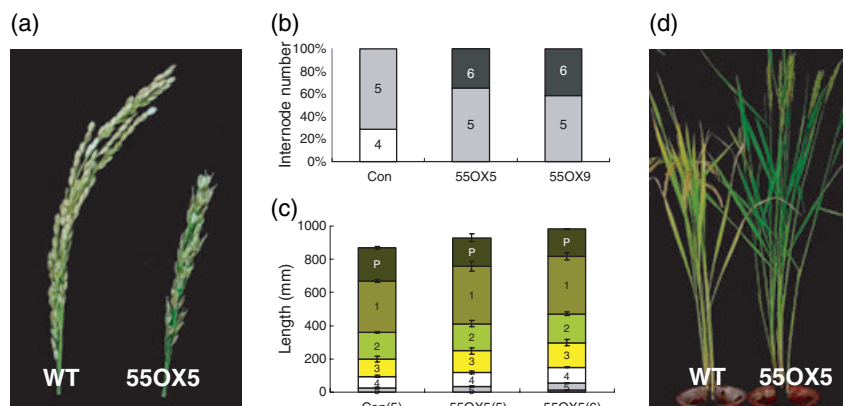
that process in rice, we tested whether its biosynthesis and the downstream genes were upregulated in RNAi plants. Two BR-biosynthesis genes were selected, *Dwarf1 (BRD1)* and *Ebisu Dwarf (Dwarf2 or D2)*, which encode BR C-6 oxidase and a cytochrome P450, respectively (Hong *et al.*, 2002, 2003). Although neither of their expression levels was significantly changed in the transgenic plants (Figure 8a,b), the two BR downstream genes, *OsBLE3* (Yang *et al.*, 2006) and *OsXTR1 (Oryza sativa xyloglucan endotransglycosylase-related 1; Uozu et al.*, 2000), were upregulated in the 55R, 2255R and 224755R plants that had increased LJ inclination (Figure 8c,d). These upregulation patterns were not observed from the *OsMADS22* knock-out plants, which showed normal patterns of LJ inclination.

The effects of SVP-group MADS-box genes in BR responses at the seedling stage

Coleoptile length and the angle of LJ inclination are increased in response to BR in rice seedlings. To understand the roles of the rice SVP-group members in these processes, we grew transgenic plants in the presence or absence of BL (1 μm), and examined whether changes in gene expression altered the BL response. This particular concentration was selected because it is the minimum needed to induce significant coleoptile elongation in the WT under continuous light conditions (Jeong *et al.*, 2007). As a positive control, the *phyB-2* mutant was used because its plants have increased BR sensitivity (Jeong *et al.*, 2007).

Figure 6. Phenotypes of transgenic plants over-expressing *OsMADS55*.

(a) Panicle morphology for wild-type (WT) and 55OX line 5.
 (b) The numbers of elongated internodes compared between 55OX plants and WT (data from 10 independent panicles).
 (c) Stem lengths for WT and 55OX plants containing five or six elongated internodes. The numbers indicate position of internodes from top; P, panicle.
 (d) WT and 55OX line 5.



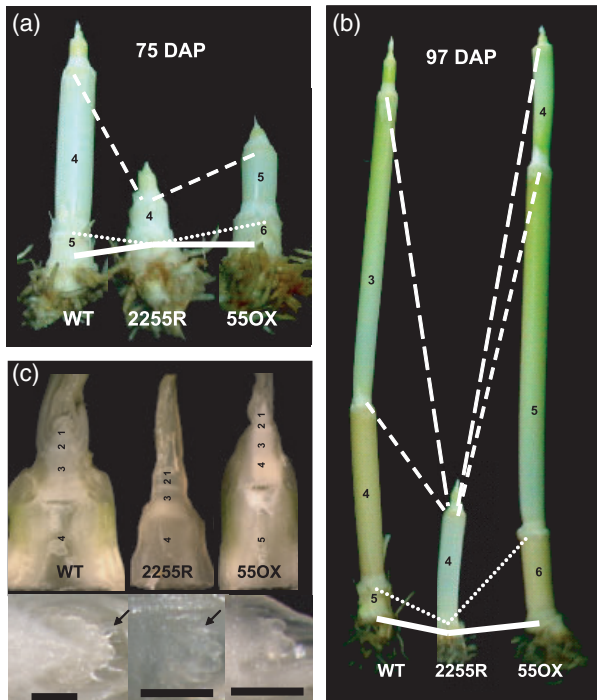


Figure 7. Stem elongation process in wild-type (WT), 2255R and 55OX plants. (a) Patterns of elongation in WT, 2255R and 55OX plants at 75 days after planting (DAP). Each internode position is indicated. (b) Stem elongation patterns in 2255R and 55OX plants at 97 DAP. (c) Dissected stems from WT, 2255R and 55OX plants at 75 DAP. The numbers indicate panicle primordia (1), and 1st (2), 2nd (3), 3rd (4), and 4th (5) internodes. Enlarged views of each panicle primordia are shown below. Scale bars: 0.5 mm. Arrows indicate bract hairs.

When BL was lacking, coleoptile lengths were the same for the transgenics and the WT (data not shown). Upon its application, however, an increase in lengths and the angle of

LJ inclination was prominent in double (2255R) and triple RNAi plants (224755R), whereas 22KO and 55R plants showed the same BL response as the WT controls (Figure 9). This indicated that both genes function together in coleoptile elongation and determining LJ inclination.

Discussion

Conserved roles for rice SVP-group MADS-box genes as modulators of meristem identity

Not only in Arabidopsis but also in barley, the SVP-group MADS-box genes induce flower abnormalities and floral reversion when overexpressed (Trevaskis *et al.*, 2007; Yu *et al.*, 2002). In this study, we confirmed a previous report that *OsMADS22* overexpressing plants develop similar phenotypes (Sentoku *et al.*, 2005). Furthermore, fertility was reduced and panicles were shorter in our plants. When we generated overexpression lines for the other SVP-group member, *OsMADS55*, we observed severe abnormalities, including reduced fertility, shortened panicles, defective flowers and floral reversion. Therefore, we can conclude that the role of these genes in meristem identity is well conserved in both monocots and dicots.

However, when only one of those genes was suppressed at a time, the flower morphology was not altered. This observation is similar to that described for Arabidopsis, in which single knock-out mutants show no such defects, whereas the double *svp agl24* mutants have fewer floral organs and display homeotic conversions of sepals to petaloid organs as a result of the ectopic expression of Class-B and -C organ identity genes (Gregis *et al.*, 2006). However, our double and triple RNAi rice flowers had no developmental defects, perhaps because of residual levels

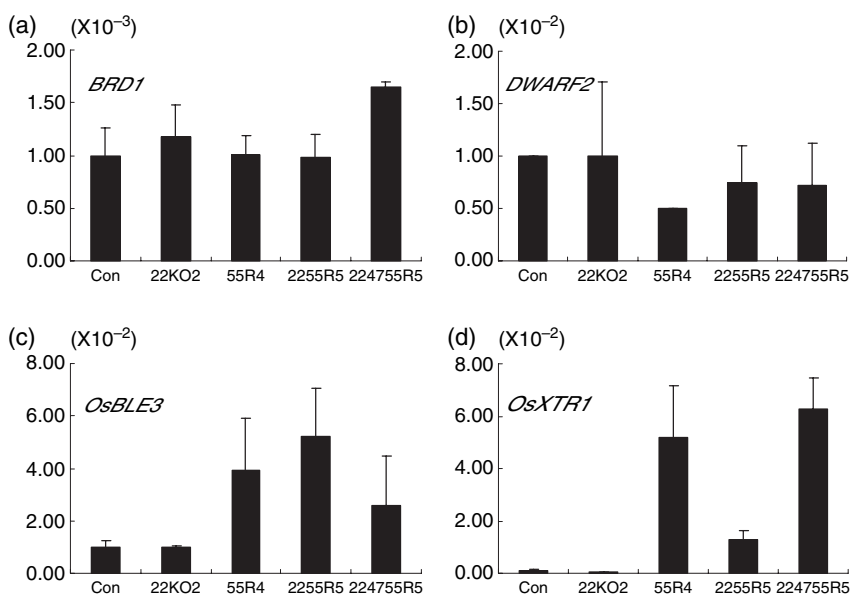
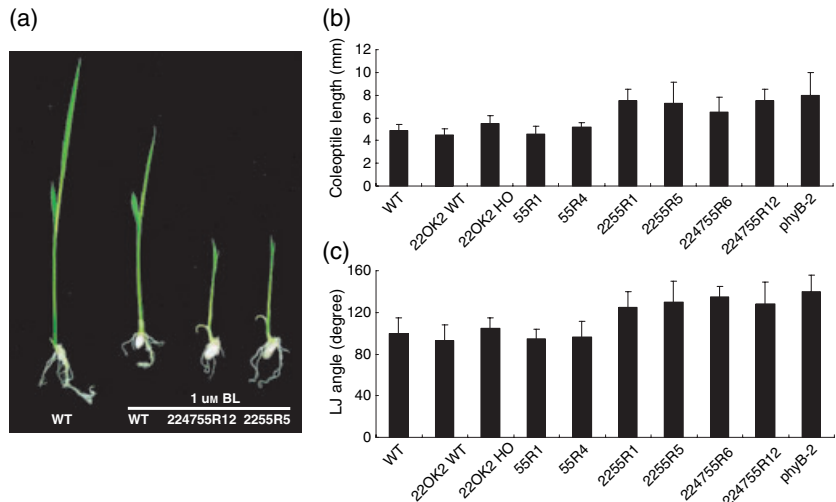


Figure 8. Transcript levels of brassinosteroid (BR)-biosynthesis genes *BRD1* (a) and *DWARF2* (b), and downstream genes *OsBLE3* (c) and *OsXTR1* (d), in 22KO, 55R, 2255R and 224755R plants. The y-axis represents the relative values between the transcript levels of target genes and the control *ubiquitin*.

Figure 9. Effects of epibrassinolide (BL) on RNAi transgenic plants. All experiments were repeated more than twice, with more than 10 plants analyzed each time.

(a) Comparison of the double or triple RNAi plants with wild-type (WT) plants grown in the presence of $1 \mu\text{M}$ BL.
 (b) Coleoptile lengths for RNAi transgenic plants grown in the presence of $1 \mu\text{M}$ BL.
 (c) Angle of lamina joint inclination from RNAi transgenic plants grown in the presence of $1 \mu\text{M}$ BL.



of gene expression that remained in the RNAi plants, or because other MADS-box genes complement the loss of the rice SVP-group genes. Alternatively, floral defects may arise only under certain environmental conditions.

Rice SVP-group MADS-box genes are not involved in controlling the time of floral transition

In plants of the double mutant 2255R and the triple mutant 224755R, the heading dates were slightly delayed, not because of alterations in the timing of floral transition, but because of the reduced stem elongation. RT-PCR analyses showed that transcript levels of flowering activators *Ehd1*, *OsMADS14* and *Hd3a* were not changed in either SD- (Figure S5) or LD-grown transgenic plants (data not shown). Those that overexpressed *OsMADS55* headed about 1-week late because of the additional internode elongation process. However, overexpression of *OsMADS22* did not change the heading date. This indicates that *OsMADS55* plays a role in regulating that date by controlling stem elongation, and that *OsMADS22* assists *OsMADS55*.

In barley, ectopic expression of *BM1* also causes a slight delay in the heading time (Trevaskis *et al.*, 2007). However, this modification is not found in plants where *BM1* or *BM10* is suppressed. Therefore, as observed from rice, the barley SVP-group MADS-box genes seem to be functionally redundant. Cold treatments induce a between two- and fourfold increase in the expression of the barley SVP-group member (Trevaskis *et al.*, 2007). In contrast, the wheat SVP-group MADS-box gene *TaVRT2* is suppressed by LD and vernalization treatments (Kane *et al.*, 2005, 2007). *TaVRT2* regulates the flowering activator *TaVRN1* by directly binding to the CArG box located on the *TaVRN1* promoter (Kane *et al.*, 2007). Therefore, monocot SVP genes appear to be functionally diversified in regulating flowering time.

OsMADS22 works as a negative regulator of BR responses

OsMADS47 has been elucidated as a negative regulator in BR responses (Duan *et al.*, 2006). Here, we used several parameters to demonstrate the roles of *OsMADS22* and *OsMADS55*. The most specific BR response in rice is an increase in LJ inclination (Maeda, 1965; Takeno and Pharis, 1982; Wada *et al.*, 1981). Another is coleoptile elongation at the seedling stage (Yamamuro *et al.*, 2000); in fact, BR-deficient rice mutants have shorter stems (Hong *et al.*, 2002, 2003, 2005; Tanabe *et al.*, 2005). A positive role for BR has been discovered in the senescence process for Arabidopsis and tomato (Altmann, 1999; Vidya Vardhini and Rao, 2002), but, until now, had not been reported for rice.

Our *OsMADS22*-overexpressing plants had shorter stems, reduced LJ inclination and delayed senescence at the mature stage, confirming that the gene acts as a negative regulator in BR responses. However, the *OsMADS22* knock-out plants did not show any change in coleoptile elongation, LJ inclination or stem elongation, probably because other SVP genes (*OsMADS47* and *OsMADS55*) compensated for the deficiency in *OsMADS22*.

OsMADS55 acts as a negative regulator of BR responses together with OsMADS22

With regard to leaf senescence, we see that *OsMADS55* works similarly to *OsMADS22* because *OsMADS55*-overproducing plants exhibit delayed senescence. However, the *OsMADS55* knock-down plants do not differ significantly in this trait, implying that the suppression of both *OsMADS22* and *OsMADS55* is needed to cause the enhanced-senescence phenotype.

In other reports of the involvement of MADS-box genes in aging-related processes, Mao *et al.* (2000), for example, has shown that when the tomato MADS-box gene *JOINTLESS* is

mutated, the resultant plants do not develop abscission zones on their pedicels (Mao *et al.*, 2000). Mutation in another tomato MADS-box gene, *LeMADS-RIN*, causes a failure in fruit-ripening (Vrebalov *et al.*, 2002). Furthermore, transgenic plants expressing sense *AGL15* have inhibited senescence programs in their perianth organs and developing fruits (Fang and Fernandez, 2002; Fernandez *et al.*, 2000). *FRUITFULL (FUL)*, *SHATTERPROOF1 (SHF1)* and *SHF2* are also involved in differentiation within the fruit dehiscence zone (Gu *et al.*, 1998). These MADS-box genes may regulate senescence-related processes via interactions with BR or ethylene signaling.

Besides during senescence, our double RNAi plants showed enhanced BR responses at the seedling stage. This synergistic effect was also noted at maturity in the LJ, where inclination was observed in the flag and second leaves of 2255R plants, whereas this phenomenon in 55R was manifested only in the first leaves. All of these results suggest a role for OsMADS55 as a negative regulator of BR responses in conjunction with OsMADS22. Furthermore, double RNAi analyses for *OsMADS47* and *OsMADS55* would be needed for examining the possibility that OsMADS47 may also support the roles of OsMADS55.

OsMADS55 controls stem elongation together with OsMADS22

The role of SVP-group genes in stem elongation can be predicted from their expression patterns. In potato, *StMADS11* and *StMADS16* are highly expressed in the stems (Carmona *et al.*, 1998; Garcia-Maroto *et al.*, 2000). For barley, *BM1* expression is strong in the nodes and internodes, where it is localized in a single-cell layer of meristematic cells in the node (Carmona *et al.*, 1998; Schmitz *et al.*, 2000). Furthermore, enhanced stem elongation is observed in *BM1*-overexpressing barley and *StMADS16*-overexpressing tobacco (Garcia-Maroto *et al.*, 2000; Trevaskis *et al.*, 2007). However, stem reductions have not been reported earlier in the knock-out or knock-down lines of these SVP-group genes. Our detailed stem analyses showed that 55R plants contained fewer elongated internodes, whereas some of the 55OX plants generated more elongated internodes. Because 2255R plants developed a lower number compared with 55R plants, the two genes appeared to function synergistically. *OsMADS22* knock-out plants did not show this phenotype, so OsMADS55 is considered the major regulator of stem elongation.

BR is a positive regulator of stem elongation, and BR-signaling and BR-biosynthesis mutants have been isolated from dwarf mutants in Arabidopsis (Asami *et al.*, 2005; Belkhadir and Chory, 2006; Choi, 2007). In rice, mutations in the BR-biosynthesis genes also cause dwarfism (Hong *et al.*, 2002, 2003, 2005; Tanabe *et al.*, 2005). However, BR oversensitivity does not always induce stem elongation. For

example, even though *bzr1-1D* plays a positive role in BR signaling, its mutant undergoes less cell elongation when grown in light (Wang *et al.*, 2002). Our analyses for rice *phyB* mutants also showed that plants were shorter at the seedling stage, whereas LJ inclination and coleoptile lengths were increased (Jeong *et al.*, 2007). Therefore, the inhibition of stem growth could have been induced by either BR insensitivity or oversensitivity. If their molecular environments were conserved between stems and LJs, OsMADS22 and OsMADS55 may have worked as negative regulators of BR responses in stems. In our study, the reductions in stem number and length in the 55R and 2255R plants may have resulted from drastic BR oversensitivity. If the stems and LJs differed considerably, then OsMADS22 and OsMADS55 might have acted as positive regulators of BR responses by forming different kinds of protein complexes. In petunia and Arabidopsis, this group of MADS-box proteins binds to various MADS-box proteins from other groups (de Folter *et al.*, 2005; Immink *et al.*, 2003).

Diversified and conserved roles for rice SVP-group genes in BR responses

Our analyses showed that OsMADS22 and OsMADS55 work as negative regulators of BR responses; however, their roles are diversified, functioning at different developmental stages. Although *OsMADS47* was expressed highly in seedling leaves, the *OsMADS55* transcript was more abundant in the mature leaves. Therefore, these expression patterns imply that OsMADS55 and OsMADS47 are the determinative negative regulators of BR responses in leaves. Clear BR-related abnormal phenotypes in the transgenic plants suppressing *OsMADS55* or *OsMADS47* also support this (Duan *et al.*, 2006). Furthermore, constitutive expression levels of *OsMADS22*, and the absence of phenotypes in single knock-out plants suggest that the latter gene plays a supporting role.

In the LJs of flag leaves from mutant plants, BR-downstream genes (*OsBLE3* and *OsXTR1*) were upregulated, whereas the two BR-biosynthesis genes (*BRD1* and *DWARF2*) were not altered significantly. This suggests that the SVP-group genes function in this BR response by competing with its downstream signaling. Because their expression levels were not altered by BL treatment, they may not be considered BR-downstream genes. One possible explanation is that the MADS proteins compete with positive response factors for inducing those downstream genes.

Experimental procedures

Plant materials and growing conditions

All transgenic lines and WT plants used here were from *O. sativa* var. *japonica* cv. Dongjin, except for the *osmads22-1* knock-out

mutant, which was var. *japonica* cv. Hwayoung. Transgenic plants were grown under confinement in a paddy field or in a glasshouse. To monitor the effect of flowering time, plants were cultured in controlled growth rooms under SD (10-h light/14-h dark) or LD (14-h light/10-h dark).

For hormonal treatments, 3-week-old plants were transferred to tap water containing the appropriate levels of hormones. BL (10 mM) and GA (10 mM) stocks were prepared by dissolving reagents in 95% alcohol and sterilized water, respectively. To test constitutive BR responses, seeds were surface-sterilized and seedlings were grown at 28°C on gauze embedded in an MS medium containing 1 µM BL.

Vector construction and transformation

The Gateway cloning system was used to construct our RNAi molecules. First, PCR products were cloned into the pGA2960 entry vector, which was generated by modifying pENTR 1A (Invitrogen, <http://www.invitrogen.com>). The fragments were then subcloned into the pANDA binary vector through an LR clonase reaction (Miki and Shimamoto, 2004). Amplified regions within the transcripts of each gene included: 749–1120 bp of *OsMADS55* cDNA (AK111859) for the OM55R plants; 361–726 bp of *OsMADS22* cDNA (AB003322) and 497–793 bp of *OsMADS55* cDNA for the OM2255R plants; and 361–726 bp of *OsMADS22* cDNA, 416–792 bp of *OsMADS47* cDNA and 497–793 bp of *OsMADS55* cDNA for the OM224755R plants. These numbers indicate the nucleotide positions from the translation initiation sites of each cDNA. Overexpression lines were generated by cloning the full-length cDNAs of *OsMADS22* and *OsMADS55* into the pGA1611 binary vector (Kim *et al.*, 2003) between the maize *Ubi* promoter and the nopaline synthase (*nos*) terminator. The rice plants were transformed according to *Agrobacterium*-mediated co-cultivation methods (Lee *et al.*, 1999).

RNA isolation, semi-quantitative RT-PCR and quantitative real-time PCR

Total RNAs were isolated with Tri Reagent (MRC Polymers Inc., <http://www.mrcpolymers.com>), following the manufacturer's instructions. First-strand cDNA was synthesized from 2 to 4 µg of total RNA, using Moloney murine leukemia virus (M-MLV) reverse transcriptase (Promega, <http://www.promega.com>), with 10 ng of the oligo (dT)15 primer and 2.5 mM deoxyribonucleotide triphosphate (dNTP). Synthesized cDNAs were used for semi-quantitative RT-PCR or real-time PCR. Real-time PCR was performed with a Roche Lightcycler II (Roche, <http://www.roche.com>); *ubiquitin* was used for normalizing the cDNA quantity. Primers included CACGGTCAACAACATCCAG' and TGAAGACCCTGACTGGGAAG for *ubiquitin*; GGAGGAGATCGGTCTCGGTCGATC and GACTTGTCGATGATTTTCATTC for *OsMADS22*; CGTCGTCTTCTCCGCCACCGGCAA and CCTGCAGCTGTTCCACATTC for *OsMADS47*; TGGAAGAGCTGCAGCAGATG and TCATCACAGATTCAGATGATTG for *OsMADS55*; CCAGCCAAGACCAAGGAG and CTGCTTAGCATGCAACAAG for *DWARF1*; TTGTGTACTTCCGGTCAGTC and CTGAGCTGGTGACCAAGTG for *DWARF2*; TGGCGCTAACACAGATGTG and ACATCGGTGACAATGTGGAG for *OsBLE3*; and CGTACATCTGCAGACGAAC and GAGTAGAGCTTCATCGGCTG for *OsXTR1*.

LJ inclination assay

Seeds were sterilized in 50% bleach for 30–50 min, depending on their status. Endosperms were then partially embedded in an MS agar medium for uniform germination. After 5 days of growth at

30°C, seedlings showing retarded development were eliminated. The others were injected, at the top of the lamina of their second leaves, with 1 µl of an ethanol solution containing 1 mM BR (Fujioka *et al.*, 1998). After incubation for 2 days, the angle was measured between the lamina and its sheath on the second leaf.

Acknowledgements

We thank Ko Shimamoto for providing the pANDA vector, Dong-Hoon Jeong for providing the *phyB* KO seeds and Priscilla Licht for her critical reading of the manuscript. This work was supported, in part, by grants from the Crop Functional Genomic Center, the 21st Century Frontier Program (Grant CG1111); from the Bio-green 21 Program (20070401-034-001-007-03-00), Rural Development Administration; and from the Korea Science and Engineering Foundation (KOSEF) through the National Research Laboratory Program funded by the Ministry of Science and Technology (M10600000270-06J0000-27010).

Supplementary material

The following supplementary material is available for this article online:

Figure S1. Expression patterns of short vegetative phase (SVP)-group MADS-box genes.

Figure S2. Characterization of *OsMADS22* knock-out (KO) plants.

Figure S3. Expression levels of the short vegetative phase (SVP)-group MADS-box genes in 2255R plants.

Figure S4. Abnormal flowers from *OsMADS55*-overproducing plants.

Figure S5. Expression patterns of flowering time regulators in 2255R and 224755R plants grown for 55 days under short-day (SD) conditions.

Table S1. Analyses of stems and lamina joints in the transgenic plants.

This material is available as part of the online article from <http://www.blackwell-synergy.com>

Please note: Blackwell Publishing are not responsible for the content or functionality of any supplementary materials supplied by the authors. Any queries (other than missing material) should be directed to the corresponding author for the article.

References

- Altmann, T. (1999) Molecular physiology of brassinosteroids revealed by the analysis of mutants. *Planta*, **208**, 1–11.
- An, S., Park, S., Jeong, D.H. *et al.* (2003) Generation and analysis of end sequence database for T-DNA tagging lines in rice. *Plant Physiol.* **133**, 2040–2047.
- Arora, R., Agarwal, P., Ray, S., Singh, A.K., Singh, V.P., Tyagi, A.K. and Kapoor, S. (2007) MADS-box gene family in rice: genome-wide identification, organization and expression profiling during reproductive development and stress. *BMC Genomics*, **8**, 242.
- Asami, T., Nakano, T. and Fujioka, S. (2005) Plant brassinosteroid hormones. *Vitam. Horm.* **72**, 479–504.
- Belkhadir, Y. and Chory, J. (2006) Brassinosteroid signaling: a paradigm for steroid hormone signaling from the cell surface. *Science*, **314**, 1410–1411.
- Carmona, M.J., Ortega, N. and Garcia-Maroto, F. (1998) Isolation and molecular characterization of a new vegetative MADS-box gene from *Solanum tuberosum* L. *Planta*, **207**, 181–188.
- Choi, S. (2007) Signal-transduction pathways toward the regulation of brassinosteroid biosynthesis. *J. Plant Biol.* **50**, 225–229.

- Doi, K., Izawa, T., Fuse, T., Yamanouchi, U., Kubo, T., Shimatani, Z., Yano, M. and Yoshimura, A. (2004) Ehd1, a B-type response regulator in rice, confers short-day promotion of flowering and controls FT-like gene expression independently of Hd1. *Genes Dev.* **18**, 926–936.
- Duan, K., Li, L., Hu, P., Xu, S.P., Xu, Z.H. and Xue, H.W. (2006) A brassinolide-suppressed rice MADS-box transcription factor, OsMDP1, has a negative regulatory role in BR signaling. *Plant J.* **47**, 519–531.
- Fang, S.C. and Fernandez, D.E. (2002) Effect of regulated over-expression of the MADS domain factor AGL15 on flower senescence and fruit maturation. *Plant Physiol.* **130**, 78–89.
- Fernandez, D.E., Heck, G.R., Perry, S.E., Patterson, S.E., Bleecker, A.B. and Fang, S.C. (2000) The embryo MADS domain factor AGL15 acts postembryonically. Inhibition of perianth senescence and abscission via constitutive expression. *Plant Cell*, **12**, 183–198.
- de Folter, S., Immink, R.G., Kieffer, M. et al. (2005) Comprehensive interaction map of the *Arabidopsis* MADS Box transcription factors. *Plant Cell*, **17**, 1424–1433.
- Fujioka, S., Noguchi, T., Takatsuto, S. and Yoshida, S. (1998) Activity of brassinosteroids in the dwarf rice lamina inclination bioassay. *Phytochemistry*, **49**, 1841–1848.
- Garcia-Maroto, F., Ortega, N., Lozano, R. and Carmona, M.J. (2000) Characterization of the potato MADS-box gene STMADS16 and expression analysis in tobacco transgenic plants. *Plant Mol. Biol.* **42**, 499–513.
- Gregis, V., Sessa, A., Colombo, L. and Kater, M.M. (2006) AGL24, SHORT VEGETATIVE PHASE, and APETALA1 redundantly control AGAMOUS during early stages of flower development in *Arabidopsis*. *Plant Cell*, **18**, 1373–1382.
- Gu, Q., Ferrandiz, C., Yanofsky, M.F. and Martienssen, R. (1998) The FRUITFULL MADS-box gene mediates cell differentiation during *Arabidopsis* fruit development. *Development*, **125**, 1509–1517.
- Hartmann, U., Hohmann, S., Nettekheim, K., Wisman, E., Saedler, H. and Huijser, P. (2000) Molecular cloning of SVP: a negative regulator of the floral transition in *Arabidopsis*. *Plant J.* **21**, 351–360.
- Hong, Z., Ueguchi-Tanaka, M., Shimizu-Sato, S. et al. (2002) Loss-of-function of a rice brassinosteroid biosynthetic enzyme, C-6 oxidase, prevents the organized arrangement and polar elongation of cells in the leaves and stem. *Plant J.* **32**, 495–508.
- Hong, Z., Ueguchi-Tanaka, M., Umemura, K., Uozu, S., Fujioka, S., Takatsuto, S., Yoshida, S., Ashikari, M., Kitano, H. and Matsuoka, M. (2003) A rice brassinosteroid-deficient mutant, *ebisu dwarf* (d2), is caused by a loss of function of a new member of cytochrome P450. *Plant Cell*, **15**, 2900–2910.
- Hong, Z., Ueguchi-Tanaka, M., Fujioka, S., Takatsuto, S., Yoshida, S., Hasegawa, Y., Ashikari, M., Kitano, H. and Matsuoka, M. (2005) The rice brassinosteroid-deficient dwarf2 mutant, defective in the rice homolog of *Arabidopsis* DIMINUTO/DWARF1, is rescued by the endogenously accumulated alternative bioactive brassinosteroid, dolichosterone. *Plant Cell*, **17**, 2243–2254.
- Immink, R.G., Ferrario, S., Busscher-Lange, J., Kooiker, M., Busscher, M. and Angenent, G.C. (2003) Analysis of the petunia MADS-box transcription factor family. *Mol. Genet. Genom.* **268**, 598–606.
- Jang, S.H., An, K., Lee, S. and An, G.H. (2002) Characterization of tobacco MADS-box genes involved in floral initiation. *Plant Cell Physiol.* **43**, 230–238.
- Jeong, D.H., An, S., Park, S. et al. (2006) Generation of flanking sequence-tag database for activation-tagging lines in japonica rice. *Plant J.* **45**, 123–132.
- Jeong, D.H., Lee, S., Kim, S.L., Hwang, I. and An, G. (2007) Regulation of brassinosteroid responses by phytochrome B in rice. *Plant Cell Environ.* **30**, 590–599.
- Kane, N.A., Danyluk, J., Tardif, G., Ouellet, F., Laliberte, J.F., Limin, A.E., Fowler, D.B. and Sarhan, F. (2005) TaVRT-2, a member of the StMADS-11 clade of flowering repressors, is regulated by vernalization and photoperiod in wheat. *Plant Physiol.* **138**, 2354–2363.
- Kane, N.A., Agharbaoui, Z., Diallo, A.O., Adam, H., Tominaga, Y., Ouellet, F. and Sarhan, F. (2007) TaVRT2 represses transcription of the wheat vernalization gene TaVRN1. *Plant J.* **51**, 670–680.
- Kim, S., Lee, S., Kim, H.J., Nam, H.G. and An, G. (2007) OsMADS51 is a short-day flowering promoter that functions upstream of Ehd1, OsMADS14, and Hd3a. *Plant Physiol.* **145**, 1484–1494.
- Kim, S.R., Lee, S., Kang, H.G., Jeon, J.S., Kim, K.M. and An, G.H. (2003) A complete sequence of the pGA1611 binary vector. *J. Plant Biol.* **46**, 211–214.
- Kojima, S., Takahashi, Y., Kobayashi, Y., Monna, L., Sasaki, T., Araki, T. and Yano, M. (2002) Hd3a, a rice ortholog of the *Arabidopsis* FT gene, promotes transition to flowering downstream of Hd1 under short-day conditions. *Plant Cell Physiol.* **43**, 1096–1105.
- Lee, S., Jeon, J.S., Jung, K.H. and An, G. (1999) Binary vector for efficient transformation of rice. *J. Plant Biol.* **42**, 310–316.
- Lee, S., Kim, J., Son, J.S. et al. (2003) Systematic reverse genetic screening of T-DNA tagged genes in rice for functional genomic analyses: MADS-box genes as a test case. *Plant Cell Physiol.* **44**, 1403–1411.
- Lee, S., Kim, J., Han, J.J., Han, M.J. and An, G. (2004) Functional analyses of the flowering time gene OsMADS50, the putative SUPPRESSOR OF OVEREXPRESSION OF CO 1/AGAMOUS-LIKE 20 (SOC1/AGL20) ortholog in rice. *Plant J.* **38**, 754–764.
- Lee, J.H., Yoo, S.J., Park, S.H., Hwang, I., Lee, J.S. and Ahn, J.H. (2007) Role of SVP in the control of flowering time by ambient temperature in *Arabidopsis*. *Genes Dev.* **21**, 397–402.
- Maeda, E. (1965) Rate of lamina inclination in excised rice leaves. *Physiol. Plant.* **18**, 813–827.
- Mao, L., Begum, D., Chuang, H.W., Budiman, M.A., Szymkowiak, E.J., Irish, E.E. and Wing, R.A. (2000) JOINTLESS is a MADS-box gene controlling tomato flower abscission zone development. *Nature*, **406**, 910–913.
- Masiero, S., Li, M.A., Will, I., Hartmann, U., Saedler, H., Huijser, P., Schwarz-Sommer, Z. and Sommer, H. (2004) INCOMPOSITA: a MADS-box gene controlling prophyll development and floral meristem identity in *Antirrhinum*. *Development*, **131**, 5981–5990.
- Michaels, S.D., Ditta, G., Gustafson-Brown, C., Pelaz, S., Yanofsky, M. and Amasino, R.M. (2003) AGL24 acts as a promoter of flowering in *Arabidopsis* and is positively regulated by vernalization. *Plant J.* **33**, 867–874.
- Miki, D. and Shimamoto, K. (2004) Simple RNAi vectors for stable and transient suppression of gene function in rice. *Plant Cell Physiol.* **45**, 490–495.
- Nam, J., Kim, J., Lee, S., An, G., Ma, H. and Nei, M. (2004) Type I MADS-box genes have experienced faster birth-and-death evolution than type II MADS-box genes in angiosperms. *Proc. Natl Acad. Sci. USA*, **101**, 1910–1915.
- Prakash, A.P. and Kumar, P.P. (2002) PkMADS1 is a novel MADS box gene regulating adventitious shoot induction and vegetative shoot development in *Paulownia kawakamii*. *Plant J.* **29**, 141–151.
- Schmitz, J., Franzen, R., Ngyuen, T.H., Garcia-Maroto, F., Pozzi, C., Salamini, F. and Rohde, W. (2000) Cloning, mapping and expression analysis of barley MADS-box genes. *Plant Mol. Biol.* **42**, 899–913.

- Sentoku, N., Kato, H., Kitano, H. and Imai, R.** (2005) OsMADS22, an STMADS11-like MADS-box gene of rice, is expressed in non-vegetative tissues and its ectopic expression induces spikelet meristem indeterminacy. *Mol. Genet. Genom.* **273**, 1–9.
- Szymkowiak, E.J. and Irish, E.E.** (2006) JOINTLESS suppresses sympodial identity in inflorescence meristems of tomato. *Planta*, **223**, 646–658.
- Takeno, K. and Pharis, R.P.** (1982) Brassinosteroid-induced bending of the leaf lamina of dwarf rice seedlings: an auxin-mediated phenomenon. *Plant Cell Physiol.* **23**, 1275–1281.
- Tanabe, S., Ashikari, M., Fujioka, S. et al.** (2005) A novel cytochrome P450 is implicated in brassinosteroid biosynthesis via the characterization of a rice dwarf mutant, dwarf11, with reduced seed length. *Plant Cell*, **17**, 776–790.
- Trevaskis, B., Tadege, M., Hemming, M.N., Peacock, W.J., Dennis, E.S. and Sheldon, C.** (2007) Short vegetative phase-like MADS-box genes inhibit floral meristem identity in barley. *Plant Physiol.* **143**, 225–235.
- Uozu, S., Tanaka-Ueguchi, M., Kitano, H., Hattori, K. and Matsuoka, M.** (2000) Characterization of XET-related genes of rice. *Plant Physiol.* **122**, 853–859.
- Vidya Vardhini, B. and Rao, S.S.** (2002) Acceleration of ripening of tomato pericarp discs by brassinosteroids. *Phytochemistry*, **61**, 843–847.
- Vrebalov, J., Ruezinsky, D., Padmanabhan, V., White, R., Medrano, D., Drake, R., Schuch, W. and Giovannoni, J.** (2002) A MADS-box gene necessary for fruit ripening at the tomato ripening-inhibitor (rin) locus. *Science*, **296**, 343–346.
- Wada, K., Marumo, S., Ikekawa, N., Morisaki, M. and Mori, K.** (1981) Brassinolide and homobrassinolide promotion of lamina inclination of rice seedlings. *Plant Cell Physiol.* **22**, 323–325.
- Wang, Z.Y., Nakano, T., Gendron, J. et al.** (2002) Nuclear-localized BZR1 mediates brassinosteroid-induced growth and feedback suppression of brassinosteroid biosynthesis. *Dev. Cell*, **2**, 505–513.
- Yamamoto, C., Ihara, Y., Wu, X., Noguchi, T., Fujioka, S., Takatsuto, S., Ashikari, M., Kitano, H. and Matsuoka, M.** (2000) Loss of function of a rice brassinosteroid insensitive1 homolog prevents internode elongation and bending of the lamina joint. *Plant Cell*, **12**, 1591–1606.
- Yang, G., Nakamura, H., Ichikawa, H., Kitano, H. and Komatsu, S.** (2006) OsBLE3, a brassinolide-enhanced gene, is involved in the growth of rice. *Phytochemistry*, **67**, 1442–1454.
- Yu, H., Xu, Y., Tan, E.L. and Kumar, P.P.** (2002) AGAMOUS-LIKE 24, a dosage-dependent mediator of the flowering signals. *Proc. Natl Acad. Sci. USA*, **99**, 16336–16341.
- Yu, H., Ito, T., Wellmer, F. and Meyerowitz, E.M.** (2004) Repression of AGAMOUS-LIKE 24 is a crucial step in promoting flower development. *Nat. Genet.* **36**, 157–161.